Available online at www.sciencedirect.com
ScienceDirect
Bioorganic & Medicinal Chemistry 15 (2007) 1323–1329
Bioorganic & Medicinal Chemistry

Paclitaxel binding to human serum albumin—Automated docking studies

Krisztina Paal,* Aliaksei Shkarupin and Laura Beckford

Faculty of Science, University of Ontario Institute of Technology, 2000 Simcoe Street North, Oshawa, Ont., Canada L1H 7K4

Received 12 August 2006; revised 1 November 2006; accepted 8 November 2006
Available online 10 November 2006

Abstract—A computational approach was used to study the interaction of the potent anticancer drug paclitaxel (Taxol®) with human serum albumin. The primary and secondary binding sites were located at the interface of subdomains IIA and IIIA, and in the cleft between domains I and III of the protein, respectively. The C13 side chain and the baccatin core of paclitaxel were found to contribute approximately equally to the binding energy at the primary site, whereas the binding mode appears to be governed by the C13 side chain.

1. Introduction

Human serum albumin (HSA),[1,2] the most abundant human plasma protein, contains a single polypeptide chain of 585 amino acids. It is largely helical and is composed of three structurally homologous domains (I, II, III). Each domain contains 10 helices; helices 1–6 form the respective subdomains A and helices 7–10 comprise subdomains B. Albumin is an important transport protein known to bind a wide variety of endogenous and exogenous compounds; the view on the number and location of distinct binding sites has constantly been evolving. Solution of the X-ray crystallographic structure of HSA[3] facilitated the location of the two major drug binding sites, site I and site II proposed originally by Sudlow et al.,[4] in subdomains IIA and IIIA of the protein, respectively.

Paclitaxel[5] (**1**, Fig. 1) is a very potent anticancer agent widely used for the treatment of ovarian and breast carcinoma, non-small cell lung cancer, and AIDS-related Kaposi's sarcoma. The ability of the molecule to interact with several proteins plays a significant role in determining its overall biological effect. Paclitaxel binding to the β-tubulin subunits results in stabilization of the microtubule polymers and leads to the arrest of the cell division cycle.[6] This interaction has been studied extensively, with particular emphasis on the bioactive conformation of the drug.[7,8] Paclitaxel binding to Bcl-2, an apoptosis regulator protein that is an additional target of the drug[9], has been studied by computational methods.[10]

Due to its hydrophobic nature paclitaxel binds to plasma proteins extensively.[11] Its interaction with human serum albumin was concluded to be non-specific[11] and of moderate affinity,[12] although other evidence indicates high-affinity binding.[13] The latter notion is further supported by observations that paclitaxel substantially affects the fluorescence of Trp214, a residue located in subdomain IIA (drug binding site I) of albumin,[14] and strongly interferes with the binding of several site I ligands.[14,15]

Plasma protein binding of drugs is of great interest as it influences their pharmacokinetic and pharmacodynamic properties, and may also lead to interference with the binding of other endogenous and/or exogenous ligands as a result of overlap of binding sites and/or conformational changes. Detailed knowledge of the paclitaxel–albumin interaction is therefore essential for the thorough understanding of the pharmacokinetic behavior of this drug and may also facilitate the design of analogues with more favorable pharmacological properties. The purpose of our studies described herein was to perform docking experiments to search for potential high-affinity paclitaxel binding sites on HSA, to obtain structural information on the drug–albumin complex, and to gain insight into the mechanism of the binding interaction.

Keywords: Automated docking; Binding site, Human serum albumin; Paclitaxel.
* Corresponding author. Tel.: +1 905 721 8668x2939; fax: +1 905 721 3304; e-mail: krisztina.paal@uoit.ca

0968-0896/$ - see front matter © 2006 Elsevier Ltd. All rights reserved.
doi:10.1016/j.bmc.2006.11.012

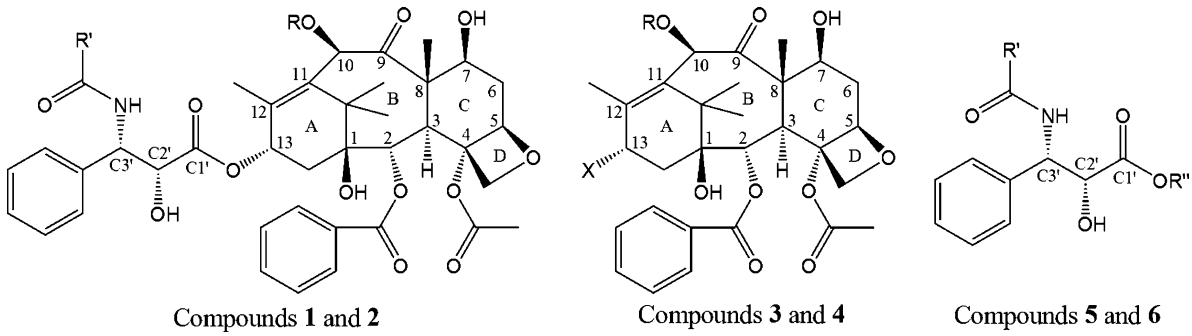

Figure 1. The ligand molecules: paclitaxel (**1**): R = CH_3CO, R′ = C_6H_5 (phenyl); docetaxel (**2**): R = H, R′ = $(CH_3)_3CO$; baccatin III (**3**): R = CH_3CO, X = OH; 13-deoxybaccatin (**4**): R = CH_3CO, X = H; C13 side chain of paclitaxel (**5**): R′ = C_6H_5 (phenyl), R″ = H; C13 side chain of paclitaxel, methylated (**6**): R′ = C_6H_5 (phenyl), R″ = CH_3.

2. Results and discussion

As an initial exploration, the entire albumin molecule was scanned by six overlapping grid maps of $126 \times 126 \times 126$ points with a spacing of 0.375 Å. The classical drug binding site I in subdomain IIA, the interface of subdomains IIA and IIIA, and the cleft between domains I and III of the protein were identified as regions of high paclitaxel binding affinity. These were then further explored by using smaller grid maps and by performing a greater number of genetic algorithm runs, as described in detail in Section 4. Our results predict that the primary paclitaxel binding site is located at the interface of subdomains IIA and IIIA with the C13 side chain of the molecule buried in drug binding site I in subdomain IIA, whereas the secondary binding site is positioned in the cleft between domains I and III (Fig. 2). These predictions are in excellent agreement with previous experimental results showing that paclitaxel substantially affects the binding of site I ligands to subdomain IIA and has a minor influence on heme binding to subdomain IB.[14,15] (The heme binding site is located in subdomain IB of HSA in the presence of five bound myristic acid molecules.[16])

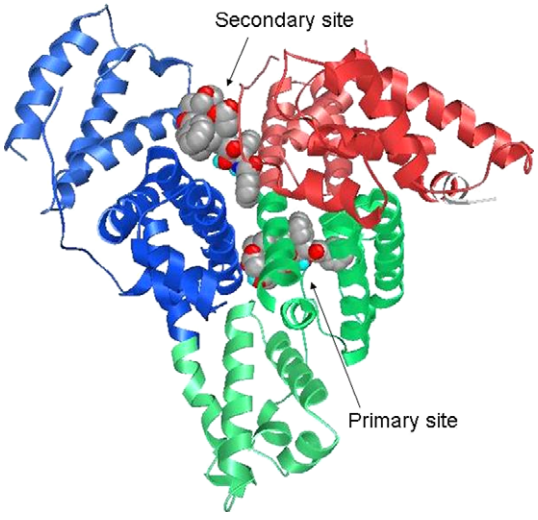

Figure 2. The primary and secondary paclitaxel binding sites on HSA (HSA: from PDB 1AO6). The protein domains are colored as follows: I, red; II, green; III, blue. The paclitaxel molecules (preferred conformations) are shown in a space-filling representation and are colored by atom type (carbon, gray; oxygen, red; nitrogen, blue).

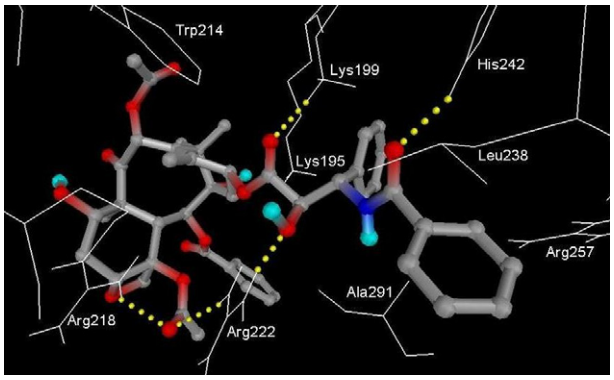

Figure 3. Paclitaxel (**1**) binding at its primary site on HSA. Hydrogen bonds are shown as yellow spheres.

Paclitaxel at its primary site (Fig. 3) interacts with subdomain IIA, the polypeptide strand connecting subdomains IIA and IIB, and subdomain IIIA. The C13 side chain of the molecule is buried in the ligand binding pocket of subdomain IIA, whereas the rigid core ring system is located at the interface of subdomains IIA and IIIA, with the bottom of the cup formed by rings A–C oriented approximately toward subdomain IIIA. Five hydrogen bond interactions were identified; three of these are contributed by the C13 side chain and two by the baccatin core of the ligand (Fig. 3, Table 1). It is interesting to note that paclitaxel was also found to make five hydrogen bonds with the same distribution between its core and its C13 side chain with amino acid residues of Bcl-2, an apoptosis regulator protein.[10] This type of interaction, on the other hand, does not appear to be crucial for tubulin binding.[7] The oxygen atoms of the C1′=O, C2′–OH, and C3′–NHCOPh groups interact with the side chains of Lys199, Arg222, and His242, respectively, whereas the carbonyl O of the C4-acetate moiety makes two hydrogen bonds with the guanidinium functional groups of Arg218 and Arg222 at the entrance to site I. The phenyl ring of C3′–NHCOPh is stacked between helices 3 and 6 of subdomain IIA, making hydrophobic contact with Leu238 and Ala291, a usual position assumed by planar groups

Table 1. Hydrogen bond interactions between ligand molecules and amino acid residues at the primary and secondary paclitaxel binding sites on HSA

Ligand[a]	Primary site			Secondary site		
	Donor	Acceptor	Distance (Å)	Donor	Acceptor	Distance (Å)
1	Lys199	O=C1′	2.2	Arg114	O–C10	2.2
	His242	O=C (C3′–NHCO–)	2.2	Leu112 (NH, bb[b])	O=C (C4–O–CO–)	1.8
	Arg222	O–C2′	1.8			
	Arg222	O=C (C4–O–CO–)	2.2			
	Arg218	O=C (C4–O–CO–)	2.1			
2	Arg218	O=C1′	1.9	Arg114	O–C1	1.8
	Arg222	O=C (C3′–NHCO–)	1.6	Arg114	O–C2	2.1
	Lys195	–O– (C3′–NHCO–O–)	2.0			
	Asn295	O–C1	1.9			
	C10–OH	Glu292 (C=O, bb)	1.9			
3	Asn295	O–C13	1.9	Arg145	O–C4	2.2
	C13–OH	Asn295 (C=O, sc)	1.9			
	Arg218	O–C13	1.8			
	Arg218	O–C4	2.1			
	Lys195	O–C5	2.1			
	Arg222	O=C (C4–O–CO–)	1.9			

[a] Ligands are as shown in Fig. 1: paclitaxel (**1**), docetaxel (**2**), baccatin III (**3**).
[b] bb, backbone; sc, side chain; the side-chain functional group of the amino acid residue is involved, unless otherwise noted.

of site I ligands.[17] The C3′–Ph group is positioned between the positively charged side chains of Arg257 and Lys195. The latter in turn is located between the phenyl rings of C3′–Ph and C2–OCOPh. Other residues in close contact (within 5 Å) with the C13 side chain are Glu153, Ser192, Gln196, Leu260, Ile290, and the edge of the Tyr150 ring. Helix 4 of subdomain IIIA (Pro447, Cys448, Asp451, and Val455), the polypeptide strand connecting subdomains IIA and IIB (Glu292, Val293, Glu294, and Asn295), as well as residues Gln221, Val343, and the edges of the Trp214 indole and the Tyr452 phenol rings take part in forming the binding pocket of the baccatin core.

The general orientation of docetaxel (**2**, Fig. 1) at the primary paclitaxel binding site is somewhat different: the bottom of the cup formed by rings A–C faces the strand connecting subdomains IIA and IIB (Fig. 4). In addition, the C13 side chain is not as deeply inserted into the ligand binding pocket of subdomain IIA; perhaps as a result of the replacement of the planar phenyl ring in the C3′–NHCOPh group with a *tert*-butoxy functionality that cannot be pinned between Leu238 and Ala291. Docetaxel also makes five hydrogen bond interactions with the protein, three of which involve the C13 side chain and amino acid residues at the entrance to site I (Table 1). The C3′–Ph group is in close proximity to Lys199, Trp214, and helix 4 of domain III (Asp451). The C3′-NHCOO*t*Bu group is surrounded by Lys199, Trp214, Ala291, Glu292, Lys195, and Arg222; the latter two residues make hydrogen bond interactions with the O atoms of C3′-NHCOO*t*Bu. Other residues forming the binding pocket of the C13 side chain include Arg218 that makes a hydrogen bond with C1′=O. The phenyl ring of the C2–OCOPh group is stacked between Pro339 and His440, though the latter is at a considerable distance (8 Å). Other residues forming the binding pocket of the ring system are those of the strand connecting

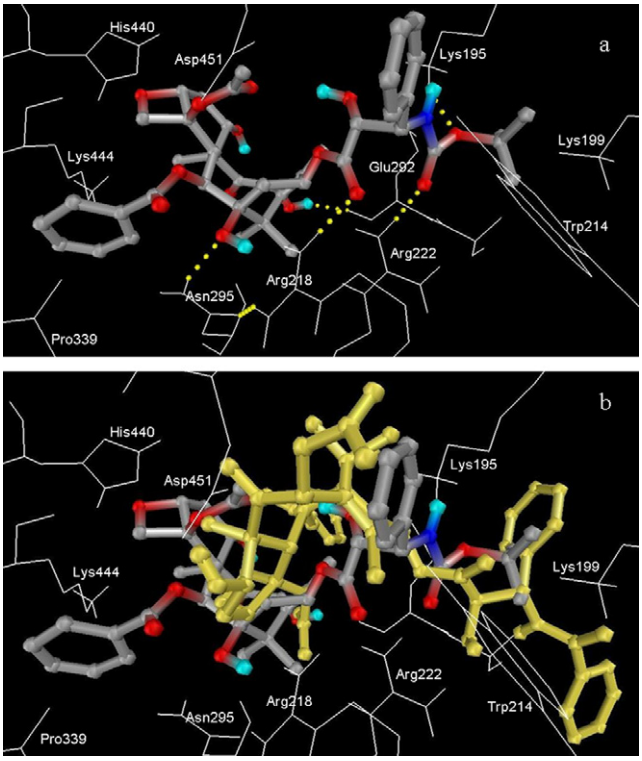

Figure 4. Preferred conformation of docetaxel (**2**) at the primary paclitaxel binding site on HSA. (a) Docetaxel alone; hydrogen bonds are shown as yellow spheres. (b) Superposition with paclitaxel (**1**, yellow).

subdomains IIA and IIB, the beginning of helix 4 of subdomain IIIA (Lys444), and the loop region between helices 8 and 9 of domain II (Pro339).

Baccatin III (**3**, Fig. 1) is too bulky to fit into site I, it resides at the interface of domains II and III of the

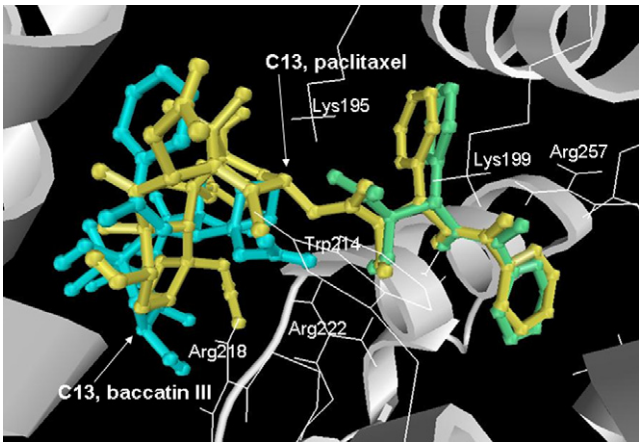

Figure 5. Preferred ligand conformations at the primary paclitaxel binding site on HSA. Paclitaxel (**1**), yellow; baccatin III (**3**), blue; C13 side chain of paclitaxel (**5**), green.

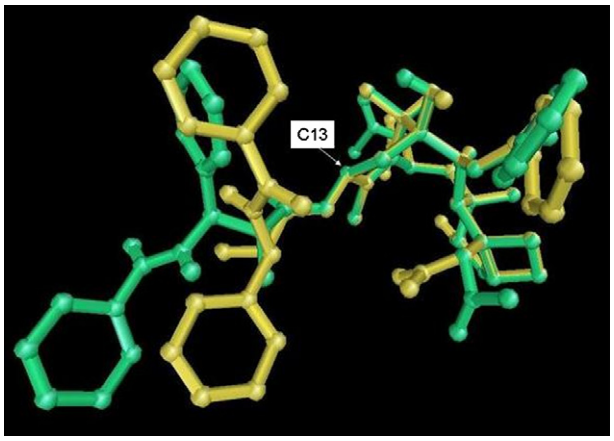

Figure 6. Superposition of paclitaxel bound to tubulin (from PDB ID 1JFF; yellow) and to its primary site on HSA (green). Prepared with MOLEKEL 4.3 (http://www.cscs.ch/molekel/).[24]

protein. This ligand occupies the same region as the ring system of paclitaxel, it is however rotated by approximately 180° (Fig. 5), causing the oxetane ring and the C4-acetate group to point toward the entrance to site I. Baccatin III makes six hydrogen bonds with the protein, involving residues Lys195, Arg218, Arg222, and Asn295 (Table 1). The C2–OCOPh phenyl ring is stacked between helix 4 of domain III and Lys195. The bottom of the cup formed by rings A–C is in close contact with helix 4 of domain III (His440, Lys444, Pro447, and Asp451), the O atom of the oxetane ring makes a hydrogen bond with Lys195, and the top of the cup interacts with subdomain IIA (helix 2 residues including Arg218, Arg222, and the edge of the Trp214 indole ring) and the polypeptide strand connecting subdomains IIA and IIB (Glu292, Val293, Glu294, and Asn295).

To further inquire into the paclitaxel binding mode at its primary site on HSA, we also docked its C13 side chain (**5**, Fig. 1) as a separate entity into the same site. Our results (Table 2) indicate that the conformation showing the best overlap with bound paclitaxel (Fig. 5) belongs to the same cluster as the preferred conformation (i.e., they represent the same binding mode of the C13 side chain). It therefore appears that the binding mode of this fragment of paclitaxel is independent of the presence/absence of the rigid core ring system. Considering that the preferred conformation of baccatin III bound at this site was found to be very different from the corresponding fragment of paclitaxel (Table 2 and Fig. 5), we can conclude that the paclitaxel binding mode is determined by the position of its C13 side chain in site I and the rest of the molecule (i.e., the core ring system) is forced to assume an otherwise unfavorable orientation at the interface of subdomains IIA and IIIA.

A comparison of the paclitaxel conformation at its primary site on HSA with the tubulin-bound conformation[7] (from PDB ID 1JFF) shows the main difference to lie in the orientation of the C13 side chain (Fig. 6). Mostly as a result of rotations about the C1′–C2′ and the C2′–C3′ bonds the entire side chain is rotated by 180° causing the two aromatic rings to switch positions. The planes of these two phenyl rings are also slightly rotated. Relatively long (9–13 Å) phenyl-to-phenyl ring distances (C2–OCOPh to C3′–Ph, and C2–OCOPh to C3′–NHCOPh) characterize both conformations, stressing the importance of the aromatic groups in maintaining interactions with the respective proteins. On the other hand, close proximity (5–6 Å) of a pair of aromatic rings—referred to as hydrophobic collapse—has been observed in both hydrophobic and polar solvents: the phenyl rings of the C2–OCOPh and C3′–Ph moieties interact in polar and those of the C2–OCOPh and C3′–NHCOPh functional groups in non-polar media.[18]

Paclitaxel and docetaxel were found to bind to the primary paclitaxel binding site of HSA with comparable affinities (Table 3); replacement of the phenyl ring in the C3′–NHCOPh group of paclitaxel with a *tert*-butoxy moiety did not significantly affect the binding energy.

Table 2. Binding energies of paclitaxel fragments at the primary paclitaxel binding site on HSA

Ligand	Binding energy (kcal/mol)		Conformations A and B in the same cluster?
	A	B	
Baccatin III (**3**)	−8.19	−6.01	No
13-Deoxybaccatin III (**4**)	−8.06	−6.45	No
C13 side chain of paclitaxel (**5**)	−9.18	−9.08	Yes
C13 side chain of paclitaxel, methylated (**6**)	−7.81	−7.24	Yes

A, preferred conformation as defined in Section 4; B, conformation showing the best overlap with the corresponding fragment of paclitaxel at its primary site on HSA.

Table 3. Ligand binding energies and binding constants at the primary and secondary paclitaxel binding sites on HSA estimated by AutoDock

Ligand	Binding energy (kcal/mol)		Binding constant (M^{-1})	
	1° Site	2° Site	1° Site	2° Site
Paclitaxel (**1**)				
Preferred conformation[a]	−11.23	−7.25	1.9×10^8	2.1×10^5
Lowest binding energy conformation[b]	—	—	—	—
Docetaxel (**2**)				
Preferred conformation	−11.49	−5.11	2.7×10^8	5.6×10^3
Lowest binding energy conformation	−11.56[c]	−7.83[c]	3.0×10^8	5.5×10^5
Baccatin III (**3**)				
Preferred conformation	−8.19	−7.05	1.0×10^6	1.5×10^5
Lowest binding energy conformation	—	−8.17	—	9.8×10^5

[a] As defined in Section 4.
[b] If different from the preferred conformation.
[c] 2×250 GA runs performed.

Complete elimination of the C13 side chain however caused a substantial decrease in the binding affinity at this site. The C13 side chains of both paclitaxel and docetaxel make three hydrogen bond interactions (Table 1) with various side chains of the protein. Interestingly, the C13-hydroxyl group of baccatin III also appears to form three hydrogen bonds with HSA. The significantly greater binding affinity of paclitaxel and docetaxel is therefore very likely to be the consequence of hydrophobic interactions between the respective C13 side chains and the protein, as well as π-cation interactions described above for the paclitaxel–albumin interaction.

In an attempt to dissect the contributions of the C13 side chain and the baccatin core of paclitaxel to the overall binding energy at the primary site, we carried out docking experiments with a methylated derivative of the C13 side chain (**6**, Fig. 1) and 13-deoxybaccatin (**4**, Fig. 1) as ligand molecules. The rationale behind the methylation at the C1′ carboxylate of the C13 side chain was to remove the negative charge and better mimic the ester functionality of paclitaxel. The C13–OH of baccatin III was deleted as the O atom is already accounted for in the methylated C13 side chain; this also eliminated hydrogen bond donor capabilities not present in paclitaxel. The predicted binding energies of the conformations of ligands **4** and **6** that show the best overlap with the corresponding fragments of paclitaxel at its primary site on HSA are −6.45 and −7.24 kcal/mol, respectively (Table 2). The sum of these two values (−13.69 kcal/mol) is somewhat smaller than the binding energy of paclitaxel (−11.23 kcal/mol; Table 3), this however can be attributed to differences in hydrogen bonding patterns (Tables 1 and 4) as well as to the somewhat different orientations of the fragments when bound alone. Most notable is the position of the C2–OCOPh phenyl ring; this group of 13-deoxybaccatin (**4**) is considerably closer to two positively charged residues (Lys436 and His440, helix 3 of subdomain IIIA) than that of paclitaxel, allowing favorable interactions of the protein with the former but not with the latter ligand. In summary, it is reasonable to conclude that

Table 4. Hydrogen bond interactions between fragments of paclitaxel and amino acid residues at the primary paclitaxel binding site on HSA

Ligand	Donor	Acceptor	Distance (Å)	Conformation[a]
Baccatin III (**3**)[b]				
13-Deoxybaccatin (**4**)	Lys195	O–C5	2.1	A
	C7–OH	Glu292 (C=O, bb[c])	2.0	A
	Arg222	O=C (C4–O–CO–)	2.0	B
C13 side chain of paclitaxel (**5**)	Lys195	$^{-}O_2C1'$	1.9, 2.0[d]	A, B
	Lys199	$^{-}O_2C1'$	1.8, 1.8	A, B
	C2′–OH	Ala291 (C=O, bb)	1.9, 2.1	A, B
	His242	O=C (C3′–NHCO–)	2.0, 1.9	A, B
	Arg222	O–C2′	2.1	B
C13 side chain of paclitaxel, methylated (**6**)	Lys199	O–C1′	2.0	A
	Arg222	O=C1′	2.2	A
	C2′–OH	Glu292	2.1	A
	Lys199	O=C (C3′–NHCO–)	2.0, 2.0	A, B
	His242	O=C (C3′–NHCO–)	1.8, 2.0	A, B
	Lys195	O=C1′	2.2	B
	Arg222	O–C2′	2.0	B

[a] Ligand conformations A and B as defined in Table 2.
[b] Hydrogen bonds of conformation A are listed in Table 1, conformation B makes no hydrogen bonds with albumin.
[c] bb, backbone; sc, side chain; the side-chain functional group of the amino acid residue is involved, unless otherwise noted.
[d] The two numbers listed refer to the complexes of conformations A and B with albumin.

the C13 side chain and the baccatin core of paclitaxel contribute to the overall ligand binding energy in an approximately equal fashion at the primary site. Similar results were previously obtained for the binding of paclitaxel to Bcl-2.[10]

The predicted binding constant at the primary paclitaxel site (Table 3) is 80-fold greater than the experimentally determined value (2.4×10^6 M^{-1}).[13] As organic solvents and solution pH affect ligand binding affinity by influencing protein conformation, most of this difference may be accounted for by variations in experimental conditions. Binding data were obtained at pH 6.5 and in the presence of ethanol,[13] whereas the crystal structure utilized for the docking studies (PDB ID 1AO6) reflects different solution conditions.[19]

The secondary paclitaxel binding site is located in the cleft between domains I and III of albumin (Fig. 2). This site significantly overlaps with the heme binding site and the secondary binding sites for several ligands.[17] The bottom of the cup formed by rings A–C of paclitaxel faces domain III and the C13 side chain of the molecule is oriented toward the interior of the protein, interacting with subdomain IB, the strand connecting subdomains IA and IB, and subdomain IIIA. Two hydrogen bond interactions with Leu112 and Arg114 were identified (Table 1). The C3′–Ph group occupies a relatively polar cavity (Asp108, Ser193, Arg197, Gln459, and Val462) and the phenyl ring of C3′–NHCOPh is surrounded by positively charged groups (His146, Arg114, Arg145, Arg186, and Lys190). Other residues forming the C13 side chain binding pocket are those of the strand connecting subdomains IA and IB (Asn109 and Pro110) and helices 3 (Glu425) and 4 (Leu463) of domain III. One side of the C2–OCOPh phenyl ring is relatively solvent exposed, and is otherwise surrounded by Asn109, Asn111, Pro421, and Lys466. The rest of the baccatin core interacts with the strand connecting subdomains IA and IB, and helix 3 of domain III. Upon examination of the heme binding site of HSA[16] (PDB ID 1N5U), residues Arg114, His146, Arg186, Lys190, and Ser193 were found to be within 5 Å from the bound heme providing a good explanation as to why paclitaxel affects the binding of this ligand to albumin.[14]

Docetaxel at the secondary site is not as deeply inserted into the protein as paclitaxel is. The orientation of the two ligands is similar in that the C13 side chain points toward the interior of albumin. Docetaxel mainly interacts with the strand connecting subdomains IA and IB, as well as subdomain IIIB. Interactions with subdomain IB and IIIA are less extensive. Two hydrogen bonds with Arg114 were identified (Table 1) along with an intramolecular hydrogen bond between C7–OH and C9=O. The C13 side chain is in close contact with the strand connecting subdomains IA and IB, and helix 3 of domain III. In particular, the C3′–Ph ring is surrounded by Asn109, Pro421, Val424, and Glu425, whereas the *t*-butyl moiety is on close proximity to Asp108, Asn109, Pro110, Leu112, Arg145, and His146. The bottom of the cup formed by rings A–C faces the solvent and the oxetane end is oriented toward helix 8 of domain III (Ile523 and Lys524). The phenyl ring of the C2–OCOPh group is stacked between Glu520 and Arg114, and is close to Lys519.

The space occupied by baccatin III at the secondary paclitaxel binding site largely overlaps with that of paclitaxel. The baccatin site is formed by the strand connecting subdomains IA and IB (Asn109, Pro110, Leu112, Arg114, and Leu115) as well as the short loop region connecting helices 8 and 9 (Arg145 and His146) and helix 10 (Arg186 and Lys190) of subdomain IB, and helices 3 (Glu425 and Asn429) and 4 (Gln459) of subdomain IIIA. One hydrogen bond interaction was identified between Arg145 and the ether O atom of the C4-acetate functionality (Table 1).

3. Conclusion

Our results presented herein provide further evidence for high-affinity binding of paclitaxel to human serum albumin. In excellent agreement with previous experimental results,[14,15] the predicted primary binding site was found to overlap with drug binding site I of HSA, whereas the secondary site is near the heme binding site. The binding mode of paclitaxel at the primary site appears to be governed by its C13 side chain, forcing the baccatin core to adopt a position that is unfavorable when this fragment is bound to the same site alone. The C13 side chain and the baccatin core were found to contribute equally to the highest-affinity binding interaction, as observed previously for the binding to Bcl-2.[10] Similarly to the tubulin-bound conformation,[7] relatively long phenyl-to-phenyl ring distances were observed in the HSA-bound paclitaxel conformations at both sites, underlining the importance of these groups in binding to albumin, and proteins in general.

4. Methods

Version 3.0.5 of AutoDock[20–22] was used for the docking studies. Paclitaxel and docetaxel structures were extracted from the protein databank (PDB) files of their X-ray crystal structures with tubulin (1JFF and 1TUB, respectively). Baccatin III, 13-deoxybaccatin, the C13 side chain of paclitaxel (methylated and non-methylated) PDB files were created in AutoDock Tools (ADT; a graphical user interface of AutoDock) by making the necessary structural changes. Ligand PDB files were imported into ADT, polar hydrogens were added, and Gasteiger charges were computed; the rigid root and the rotatable bonds were defined by the AutoTors tool of ADT. The HSA X-ray crystal structure 1AO6 was utilized for the docking experiments. The PDB file was imported into ADT, all water molecules were removed, Kollman charges and solvation parameters were added. Grid maps of $90 \times 90 \times 90$ points with a grid-point spacing of 0.375 Å were generated using the AutoGrid tool of ADT. The maps were centered on His242 (HE2[†])

[†] Atom identification used by ADT

and Arg114 (HH22[1]) for the primary and the secondary binding sites of paclitaxel, respectively. 250 Genetic Algorithm (GA) runs were performed with the following parameters: population size of 50, maximum number of 2.5×10^5 energy evaluations, maximum number of 27,000 generations, an elitism of 1, a mutation rate of 0.02, and a crossover rate of 0.8. The resulting conformations were clustered using a root-mean-square deviation (rmsd) of 2.0 Å and the clusters were ranked in order of increasing binding energy of the lowest binding energy conformation in each cluster. The most populated of the first five clusters[23] was selected for further analysis; the lowest binding energy conformation of this cluster is referred to as the preferred conformation and is described in Section 2.

Acknowledgments

The authors thank Dr. Fedor Naumkin for useful discussions and Chris Thompson for technical assistance.

References and notes

1. Peters, T. J. *All About Albumin: Biochemistry, Genetics, and Medical Applications*; Academic Press: San Diego CA, 1996.
2. Carter, D. C.; Ho, J. X. *Adv. Protein Chem.* **1994**, *45*, 153–203.
3. He, X. M.; Carter, D. C. *Nature* **1992**, *358*, 209–215.
4. Sudlow, G.; Birkett, D. J.; Wade, D. N. *Mol. Pharmacol.* **1976**, *12*, 1052–1061.
5. Spencer, C. M.; Faulds, D. *Drugs* **1994**, *48*, 794–847.
6. Schiff, P. B.; Fant, J.; Horwitz, S. B. *Nature* **1979**, *277*, 665–667.
7. Lowe, J.; Li, H.; Downing, K. H.; Nogales, E. *J. Mol. Biol.* **2001**, *313*, 1045–1057.
8. Alcaraz, A. A.; Mehta, A. K.; Johnson, S. A.; Snyder, J. P. *J. Med. Chem.* **2006**, *49*, 2478–2488.
9. Rodi, D. J.; Janes, R. W.; Sanganee, H. J.; Holton, R. A.; Wallace, B. A.; Makowski, L. *J. Mol. Biol.* **1999**, *285*, 197–203.
10. Wu, J. H.; Batist, G.; Zamir, L. O. *Anticancer Drug Des.* **2000**, *15*, 441–446.
11. Kumar, G. N.; Walle, U. K.; Bhalla, K. N.; Walle, T. *Res. Commun. Chem. Pathol. Pharmacol.* **1993**, *80*, 337–344.
12. Purcell, M.; Neault, J. F.; Tajmir-Riahi, H. A. *Biochim. Biophys. Acta* **2000**, *1478*, 61–68.
13. Paal, K.; Muller, J.; Hegedus, L. *Eur. J. Biochem.* **2001**, *268*, 2187–2191.
14. Trynda-Lemiesz, L. *Bioorg. Med. Chem.* **2004**, *12*, 3269–3275.
15. Trynda-Lemiesz, L.; Luczkowski, M. *J. Inorg. Biochem.* **2004**, *98*, 1851–1856.
16. Wardell, M.; Wang, Z.; Ho, J. X.; Robert, J.; Ruker, F.; Ruble, J.; Carter, D. C. *Biochem. Biophys. Res. Commun.* **2002**, *291*, 813–819.
17. Ghuman, J.; Zunszain, P. A.; Petitpas, I.; Bhattacharya, A. A.; Otagiri, M.; Curry, S. *J. Mol. Biol.* **2005**, *353*, 38–52.
18. Jimenez-Barbero, J.; Amat-Guerri, F.; Snyder, J. P. *Curr. Med. Chem. Anticancer Agents* **2002**, *2*, 91–122.
19. Sugio, S.; Kashima, A.; Mochizuki, S.; Noda, M.; Kobayashi, K. *Protein Eng.* **1999**, *12*, 439–446.
20. Goodsell, D. S.; Olson, A. J. *Proteins* **1990**, *8*, 195–202.
21. Morris, G. M.; Goodsell, D. S.; Huey, R.; Olson, A. J. *J. Comput. Aided Mol. Des.* **1996**, *10*, 293–304.
22. Morris, G. M.; Goodsell, D. S.; Halliday, R. S.; Huey, R.; Hart, W. E.; Belew, R. K.; Olson, A. J. *J. Comput. Chem.* **1998**, *19*, 1639–1662.
23. Källblad, P.; Mancera, R. L.; Todorov, N. P. *J. Med. Chem* **2004**, *47*, 3334–3337.
24. Flükiger, P.; Lüthi, H. P.; Portmann, S.; Weber, J. Swiss Center for Scientific Computing: Manno (Switzerland), 2000.